OXFORD

ORIGINAL ARTICLE

# Early Developmental Trajectories of Functional Connectivity Along the Visual Pathways in Rhesus Monkeys

Z. Kovacs-Balint[1], E. Feczko[1,2,3], M. Pincus[1], E. Earl[4],
O. Miranda-Dominguez[4], B. Howell[1,2], E. Morin[1,2], E. Maltbie[1], L. LI[5],
J. Steele[1], M. Styner[6], J. Bachevalier[1,7], D. Fair[4] and M. Sanchez[1,2]

[1]Yerkes National Primate Research Center, Emory University, Atlanta, GA 30329, USA, [2]Department of Psychiatry & Behavioral Science, Emory University, Atlanta, GA 30322, USA, [3]Department of Medical Informatics & Clinical Epidemiology, Oregon Health & Science University, Portland OR 97239, USA, [4]Department of Behavioral Neuroscience, Oregon Health & Science University, Portland, OR 97239, USA, [5]Department of Pediatrics, Emory University, Atlanta, GA 30322, USA, [6]Department of Psychiatry, University of North Carolina, Chapel Hill, NC 27514, USA and [7]Department of Psychology, Emory University, Atlanta, GA 30322, USA

Address correspondence to Zsofia Kovacs-Balint, Yerkes National Primate Research Center, Emory University, 954 Gatewood Road, Atlanta, GA 30329, USA. Email:zkovacs@emory.edu

## Abstract

Early social interactions shape the development of social behavior, although the critical periods or the underlying neurodevelopmental processes are not completely understood. Here, we studied the developmental changes in neural pathways underlying visual social engagement in the translational rhesus monkey model. Changes in functional connectivity (FC) along the ventral object and motion pathways and the dorsal attention/visuo-spatial pathways were studied longitudinally using resting-state functional MRI in infant rhesus monkeys, from birth through early weaning (3 months), given the socioemotional changes experienced during this period. Our results revealed that (1) maturation along the visual pathways proceeds in a caudo-rostral progression with primary visual areas (V1–V3) showing strong FC as early as 2 weeks of age, whereas higher-order visual and attentional areas (e.g., MT–AST, LIP–FEF) show weak FC; (2) functional changes were pathway-specific (e.g., robust FC increases detected in the most anterior aspect of the object pathway (TE–AMY), but FC remained weak in the other pathways (e.g., AST–AMY)); (3) FC matures similarly in both right and left hemispheres. Our findings suggest that visual pathways in infant macaques undergo selective remodeling during the first 3 months of life, likely regulated by early social interactions and supporting the transition to independence from the mother.

Key words: macaque, neurodevelopment, resting state functional MRI, social visual engagement

## Introduction

Social deficits are common across neurodevelopmental psychiatric disorders, including autism spectrum disorder (ASD), schizophrenia and social anxiety disorder (American Psychiatric Association 2013). In ASD, social deficits including the processing of social cues from faces (Klin et al. 2002, 2009; Seltzer et al. 2003),

as well as impaired social visual engagement and developmental transitions (Klin et al. 2009, 2015) are rooted in early childhood. Understanding the neurodevelopmental correlates of these impairments requires first examining the typical developmental trajectories of social skills and their neural circuitry in infancy. Social brain systems include interconnected perceptual-representation in brain areas that become attuned to salient, species-typical social signals during development (Scott et al. 2007). These early responses to social stimuli provide scaffolding for the maturation of more complex social skills (perception of biological motion and of emotions, gaze following, emotional valence attribution, etc.). Although the brain networks supporting early developing visual social skills are still unknown, work in adult monkeys have demonstrated at least 3 cortical networks: the ventral object pathway mediating facial expression and identity perception, discrimination and recognition (Ungerleider and Bell 2011); the motion pathway along the superior temporal sulcus mediating body, facial, and eye motion perception (Baylis et al. 1987; Boussaoud et al. 1990; Furl et al. 2012); and the dorsal cortical stream mediating attention/visuo-spatial processing (Ungerleider and Mishkin 1982; Dickinson et al. 2003; Liu et al. 2010). The development of these 3 visual networks has not been specifically investigated in human infants, but neuroimaging measures of white matter development in early infancy have shown exponential maturation of temporal, parietal, and frontal cortical regions during the first 2 years of age (Knickmeyer et al. 2008; Deoni et al. 2011, 2016; Geng et al. 2012; Dean et al. 2014; O'Muircheartaigh et al. 2014). Similarly, more recent studies using resting state functional MRI (rs-fMRI) have shown that sensory networks, including those in the temporal cortical areas, are the earliest developing functional networks in neonates (Lin et al. 2008; Gao et al. 2009, 2015), whereas higher-order cortical processing regions critical for social perception and emotional processing, such as the superior temporal regions and anterior cingulate cortex, do not reach adult-like topology until 2 years of age (Gao et al. 2009, 2015). Finally, the prefrontal cortex, critical for attention, memory and executive functions, continues to develop structurally and functionally throughout childhood and adolescence (Casey et al. 2000).

Given the limited knowledge on the maturation of the visual cortical pathways supporting the development of early social visual engagement and the ethical and technical limitations of frequent longitudinal neuroimaging in human infants, there is a great need to develop animal models that share important similarities with human social and neural development. Rhesus monkeys (Macaca mulatta) provide a remarkable translational opportunity due to their biological and phylogenetic closeness to humans, including the complex social behaviors and environments they experience, and the parallels in brain and social development between the two species (Preuss 2000; Machado and Bachevalier 2003; Suomi 2006; Passingham 2009; Parr 2011; Damon et al. 2017). Importantly, our recent behavioral findings also support phylogenetically conserved developmental changes in visual engagement patterns in infant macaques from 1 to 24 weeks postnatally (Muschinski et al. 2016; Parr et al. 2016; Wang et al. 2017) comparable to those reported in human infants from 2 to 6 months (Klin et al. 2015). Similarly, at the neural level, earlier histological, electrophysiological, and metabolic studies in infant monkeys have shown that cortical areas along the 3 visual streams described above mature progressively during the first 4 months after birth, from the most posterior occipital areas towards the most anterior temporal and parietal areas (Rodman et al. 1991; Webster et al.

1991; Distler et al. 1996). Moreover, a recent study showed that the adult-like hierarchical retinotopic organization of cortical areas within the ventral and dorsal visual streams was already present at birth in macaques. Yet, category selectivity within the visual cortical areas, such as selectivity for faces or scenes, emerged later during the first postnatal months, suggesting further anatomical and functional refinement as a result of postnatal visual experience (Arcaro and Livingstone 2017).

In the current study, rs-fMRI was used to examine postnatal developmental changes in infant rhesus monkeys by measuring functional connectivity (FC) between cortical regions along each pathway, based on measures of temporal correlations of blood oxygen-level dependent (BOLD) signal/activity between those regions. To achieve our goal of understanding the postnatal functional development of the 3 visual cortical streams, infant macaques were scanned longitudinally from 2 weeks through 3 months (i.e., the beginning of weaning, Suomi 2005). Also, given the criticality of normal social experience for postnatal functional refinement of the visual cortical areas, the infants were reared with their mothers in large social groups and showed behavioral shifts in the way they process social visual stimuli during the first few weeks and months of life during eye-tracking paradigms (Muschinski et al. 2016; Parr et al. 2016; Wang et al. 2017).

## Materials and Methods

### Subjects

Ten male infant rhesus monkeys were studied as part of a larger project that also examined developmental trajectories of face processing abilities using eye-tracking approaches. Subjects lived with their mothers and families in large social groups preserving critical species-specific social experiences at the Yerkes National Primate Research Center (YNPRC) Field Station, in Lawrenceville, GA (RRID: SCR_001 914). The groups were housed in outdoor compounds, with access to a climate-controlled indoor housing area. Standard high fiber, low fat monkey chow (Purina Mills Int., Lab Diets, St. Louis, MO) and seasonal fruits and vegetables were provided twice daily, in addition to enrichment items. Water was available ad libitum. Exclusionary criteria included: (1) infants of primiparous females and/or females with histories of infant physical abuse or neglect, (2) infants from the highest and lowest social hierarchy-ranked families to control for potential developmental effects of extreme social dominance status, and (3) infant birth weight <450 g, to avoid confounding effects of prematurity/low birth weight on brain development (Scott et al. 2016). Additional rsfMRI data (1) from a group of adolescent male macaques ($n = 4$, 4.46 ± 0.07 yrs) reared under similar social conditions as the infants and scanned following similar MRI protocols, were included as a reference of more mature neurocircuits for infant findings; and (2) from adults ($n = 2$ females, 12.67 ± 0.12 yrs) scanned under anesthesia and awake (after substantial training) following a within-subject design and analyzed using similar methods used in the infants, were also included to provide information on the effects of anesthesia on FC along these pathways. Although ideally we would had acquired the infants' scans awake, training socially housed infants for awake scans is not currently possible. All procedures were approved by the Emory University Institutional Animal Care and Use Committee (IACUC) in accordance with the Animal Welfare Act and the U.S. Department of Health and Human Services "Guide for Care and Use of Laboratory Animals." The YNPRC is fully accredited by AAALAC International.

## Structural MRI and rs-fMRI Image Acquisition

Neuroimaging data were collected from the infants longitudinally at 2, 4, 8, and 12 weeks of postnatal age (see Table 1 for detailed age in days and sample demographics); data from the reference group of adolescent and adult animals were acquired at 4.46 ± 0.07 and 12.67 ± 0.12 yrs, respectively, using a 3 T Siemens Magnetom Trio Tim system scanner (Siemens Med. Sol., Malvern, PA, USA), and an 8-channel phase array coil. Infants were transported with their mother from their social groups to the YNPRC Imaging Center on the day of the scan or the day before. Data were acquired during a single session, which included T1- and T2-weighted structural scans for registration purposes, and two 15-minute rs-fMRI (T2*-weighted) scans to measure temporal changes in regional BOLD signal. All animals were scanned supine in the same orientation, achieved by placement and immobilization of the head in a custom-made head holder via ear bars and a mouthpiece. A vitamin E capsule was placed on the right temple to mark the right side of the brain. Following initial telazol induction (infants: 2.89 ± 0.60 mg/kg BW, i.m; adolescents: 3.86 ± 0.02 mg/ kg BW; adults: 4.07 ± 0.03 mg/kg BW for the anesthesia condition) and intubation to minimize motion artifacts, scans were collected under anesthesia that was kept at the lowest level possible (isoflurane 0.8–1% to effect; inhalation) to minimize effects of anesthesia on BOLD signal. This range of isoflurane is below that used in previous macaque publications reporting patterns of coherent BOLD fluctuations and similar to those observed in awake and behaving monkeys, including sensory, motor, visual and cognitive-task related systems (Vincent et al. 2007; Hutchison et al. 2013; Li et al. 2013; Miranda-Dominguez 2014b; Tang and Ramani 2016). Physiological parameters were monitored using an oximeter, ECG, rectal thermistor, and blood pressure monitor. An i.v. catheter was also used to administer dextrose/NaCl (0.45%) to maintain normal hydration, and an MRI-compatible heating pad helped maintain the subjects' body temperature. Upon completion of the scans and full recovery from anesthesia, each infant was returned to its mother and the pair returned to their social group on the following day.

*Structural MRI acquisition*: High-resolution T1-weighted structural scans were acquired for registration of the functional scans using a 3D magnetization prepared rapid gradient echo (3D-MPRAGE) parallel image sequence (infants: TR/TE = 2600/ 3.46ms, FoV: 116 mm, voxel size: 0.5 mm$^3$ isotropic, 8 averages, GRAPPA, R = 2). T2-weighted MRI scans were collected in the same direction as the T1 (infants: TR/TE = 3200/373ms, FoV: 128 mm, voxel size: 0.5 mm$^3$ isotropic, 3 averages, GRAPPA, R = 2) to aid with registration and delineation of anatomical borders. The same scanning sequences were used for adolescents/adults, except for the T1 (TR = 3.38ms, and FOV = 128 mm).

*Rs-fMRI acquisition*: BOLD-weighted functional images were collected using a T2*-weighted gradient-echo echoplanar imaging (EPI) sequence (infants: 400 volumes, TR/TE = 2060/25ms, voxel size: 1.5 mm$^3$ isotropic; adolescents/adults: similar sequence but TR = 2290 ms for adolescents and 200 volumes, TR/TE = 3000/32ms for adults (Maltbie et al. 2017)) to analyze FC between brain regions. The rs-fMRI scans were collected following the T1-MRI scan (which lasted approximately 30 min) to standardize time from initial anesthesia to 45 min for all animals. An additional short, reverse-phase encoding scan was also acquired for unwarping distortions in the EPI scans using previously validated methods (Andersson et al. 2003). The first 3 volumes were removed from each EPI scan to allow for scanner equilibrium, resulting in a total of 794 concatenated volumes.

## Functional MRI Data Pre-processing

All imaging data was pre-processed similarly for normalization and comparison purposes using the FMRIB Software Library (FSL, Oxford, UK, RRID: SCR_002 823; Smith et al. 2004; Woolrich et al. 2009), 4dfp tools, and an in-house pipeline built using Nipype (Gorgolewski et al. 2011) with modifications of published methods (Fair et al. 2007, 2009, 2012; Iyer et al. 2013; Miranda-Dominguez 2014a), including some adapted for the rhesus monkey brain (Miranda-Dominguez, Mills, Grayson et al. 2014; Godfrey et al. 2018). As part of the noise and artifact reducing procedures, after file conversion, functional imaging series were: (1) unwarped using a reverse phase-encoding distortion correction method (TOPUP correction, Andersson et al. 2003), (2) slice-time corrected (for the even vs. odd slice intensity differences due to interleaved acquisition), (3) motion-corrected (rigid body motion correction within-run, linear registration from EPI to T1, and nonlinear registration from T1 to template applied all in one resampling step), and (4) normalized (signal normalization to a whole brain mode value gradient of 1000 was done to scale the BOLD values across subjects at an acceptable range to perform the rest of pre-processing steps). After the EPI functional time series were concatenated and rigid-body co-registered to the subject's averaged T1-weighted structural image, the T1-weighted structural

**Table 1.** Sample demographics and scan ages in days per subject

| ID | Cohort | Social rank | Scan age (days) 2 weeks | Scan age (days) 4 weeks | Scan age (days) 8 weeks | Scan age (days) 12 weeks |
|---|---|---|---|---|---|---|
| 1 | 2013 | 12 of 13 | 14 | 32 | 54 | 82 |
| 2 | 2014 | 8 of 11 | 17 | 31 | 59 | 87 |
| 3 | 2014 | 4 of 8 | 18 | 32 | 59 | 88 |
| 4 | 2014 | 7 of 12 | 14 | 27 | 55 | 83 |
| 5 | 2014 | 6 of 11 | 16 | 30 | 58 | 86 |
| 6 | 2015 | 9 of 13 | 15 | 28 | 55 | 83 |
| 7 | 2015 | 3 of 13 | 17 | 32 | 59 | 82 |
| 8 | 2015 | 6 of 13 | 14 | 29 | 56 | 79 |
| 9 | 2015 | 7 of 11 | 15 | 30 | 57 | 85 |
| 10 | 2015 | 10 of 11 | 14 | 26 | 56 | 83 |
| Average | | | 15.4 | 29.7 | 56.8 | 83.8 |
| S.E.M. | | | 0.5018 | 0.7209 | 0.6246 | 0.8999 |

images were transformed to conform to age-specific T1-weighted rhesus infant brain structural MRI atlases developed by our group (publicly available at: https://www.nitrc.org/projects/macaque_atlas/, Shi et al. 2017) using nonlinear registration methods in FSL (FNIRT). These infant atlases were previously registered to the 112RM-SL atlas (publicly available at: http://brainmap.wisc.edu/monkey.html) in F99 space (McLaren et al. 2009, 2010) and were templates of scans acquired longitudinally at 2 and 12 weeks of age on 40 infant rhesus monkeys from the YNPRC social colony, balanced by sex and social rank. Based on best match of neuro-anatomical characteristics, we registered the earliest scan ages (2, 4 weeks) to the 2 weeks atlas, and the later ages (8, 12 weeks) to the 12 weeks atlas. Both the 2- and the 12-weeks atlases were transformed to conform to the T1-weighted 112RM-SL atlas image in F99 space, following previously described protocols (Miranda-Dominguez et al. 2014a,b) and allowing the EPI images to be transformed into F99 space in one interpolation step for the region of interest (ROI) analysis (see below). The adolescents/adults' T1-weighted structural images were registered directly to the T1-weighted 112RM-SL atlas in F99 space and processed following similar approaches as for infants (except for using field map distortion correction in adults).

Additional pre-processing steps included: (1) functional signal detrending; (2) nuisance regressor removing (i.e., regression of rigid body head motion parameters in 6 directions, regression of the global whole-brain signal, regression of the ventricular and white matter functional signal (averaged from a ventricle- and a white matter mask, respectively), and regression of the first-order derivatives for the whole brain, ventricular and white matter signals); and (3) temporal low-pass filtering ($f < 0.1\,Hz$) via second order Butterworth filter (Fair et al. 2007, 2009, 2012; Miranda-Dominguez et al. 2014b). Global signal regression (GSR) was applied based on current literature that highlights the importance of removing systematic artifacts in the data, such as global artifacts originated not just from movement, but from respiratory and other physiological noises (Yan et al. 2013; Burgess et al. 2016; Ciric et al. 2017; Nalci et al. 2017; Power et al. 2017), including studies of the visual cortex (Power et al. 2017), and in macaque rs-fMRI studies of FC (Miranda-Dominguez 2014b; Grayson et al. 2016). Without GSR, spurious artifacts ensue, which can be particularly problematic in longitudinal studies of brain functional development, such as this one. Despite these arguments in favor of GSR, and given the controversy still existent in the field (Murphy and Fox 2017), we also ran our analyses without GSR for comparison, obtaining similar findings (data not shown). Analyses were conducted with the removal of frames with displacement (FD) value greater than 0.2 mm (Power et al. 2012, 2014). Additionally, all imaging data were visually inspected upon pre-processing completion to exclude series with unsatisfactory co-registration or significant BOLD signal dropout.

## Functional Connectivity (FC) Analysis

First, FC was analyzed between cortical ROIs along each pathway (i.e., pathway specific ROI–ROI FC analysis): (1) ventral object pathway [between: visual areas V1–V3; inferior temporal areas TEO–TE; TE-Amygdala (AMY)], (2) ventral motion pathway [between: V1 and V3; Middle Temporal area (MT) – Anterior Superior Temporal area (AST) – i.e., MT–AST-; AST–AMY] and (3) dorsal attention/visuo-spatial pathways (between: V1 and V3; Lateral Intraparietal area (LIP) – frontal eye-field (FEF) – i.e., LIP–FEF-; LIP – dorsolateral prefrontal cortex (dlPFC) Brodmann

Area 46 – i.e., LIP–BA46-). See diagrams of these pathways and ROIs in Figures 1A, 2A, and 3A. Second, a network-level analysis was conducted along each pathway to identify global, pathway-specific FC changes during development (see Figs 1B, 2B and 3B).

ROIs were defined based on the combined Lewis and Van Essen (2000) and Markov et al. (2014) published anatomical parcellations mapped onto the cortical surface of the UNC-Emory rhesus infant atlases (Shi et al. 2017) registered to the F99 space. The left and right amygdala label maps were manually drawn by experts using cytoarchitectonic maps in the existing UNC-Wisconsin adolescent atlas (RRID: SCR_002 570; Styner et al. 2007), and then propagated to the UNC-Emory rhesus infant atlases in F99 space, using deformable registration via ANTS (for details see Shi et al. 2017). Each ROI was then manually edited in the infant and the adult macaque F99 atlases separately following established anatomical landmarks (Paxinos et al. 1999; Saleem and Logothetis 2012) for neuroanatomical accuracy and to avoid (1) ROI overlap and (2) voxels with signal dropout (non-brain tissue signal).

The rs-fMRI BOLD time series were then correlated ROI by ROI (as defined in the structural atlases) for each subject and age separately. For this, the time course of the BOLD signal was averaged across the voxels within each ROI, and then correlated with the time course of the other ROIs. Correlation (FC) matrices from the aforementioned ROIs were calculated within each pathway for each age (i.e., for each subject we had one correlation/FC matrix per age). Correlation coefficients (r-values) between ROIs along each pathway of interest (i.e., ROI–ROI FC for the ventral object pathway: V1–V3, TEO–TE, TE–AMY; for ventral motion pathway: V1–V3, V3–MT, MT–AST, AST–AMY; and for the dorsal attention/visuo-spatial pathways: V1–V3, V3–LIP, LIP–BA46, LIP–FEF) were extracted from these correlation matrices using Matlab (MathWorks Inc., Natick, MA, RRID: SCR_001 622), and then Fisher Z-transformed to stabilize variance. Network analysis was also performed in Matlab, but global FC developmental changes were examined per pathway entering all ROIs at once (see details below, under Statistical Analysis).

## Experimental Design and Statistical Analysis

This study included 10 socially-housed male infant rhesus monkeys scanned longitudinally (at 2, 4, 8 at 12 weeks of age) for collection of developmental rsfMRI data following a within-subject design, as well as a group of adolescent males scanned only once (at 4.5 years of age) for comparison with infant data and 2 adult females to compare FC under anesthesia and awake state in these pathways. Only male infants were included to avoid further reducing our already moderate sample size in order to provide enough statistical power for these initial studies in macaques, particularly given the potential sex differences in brain development. The selection of males and not females for these studies was based on the focus on characterization of normative development of visual engagement neural networks of relevance for ASD-related early social deficits, given that ASD prevalence rates are 4 times greater in males than females.

Since this is the first FC study on the development of the socio-visual pathways using rsfMRI in infant macaques, no statistical methods were used to predetermine sample size. The sample size of $n = 10$ was selected based on a previous developmental diffusion tensor imaging (DTI) study in infant rhesus monkeys by our group (Howell et al. 2013), where the effect size
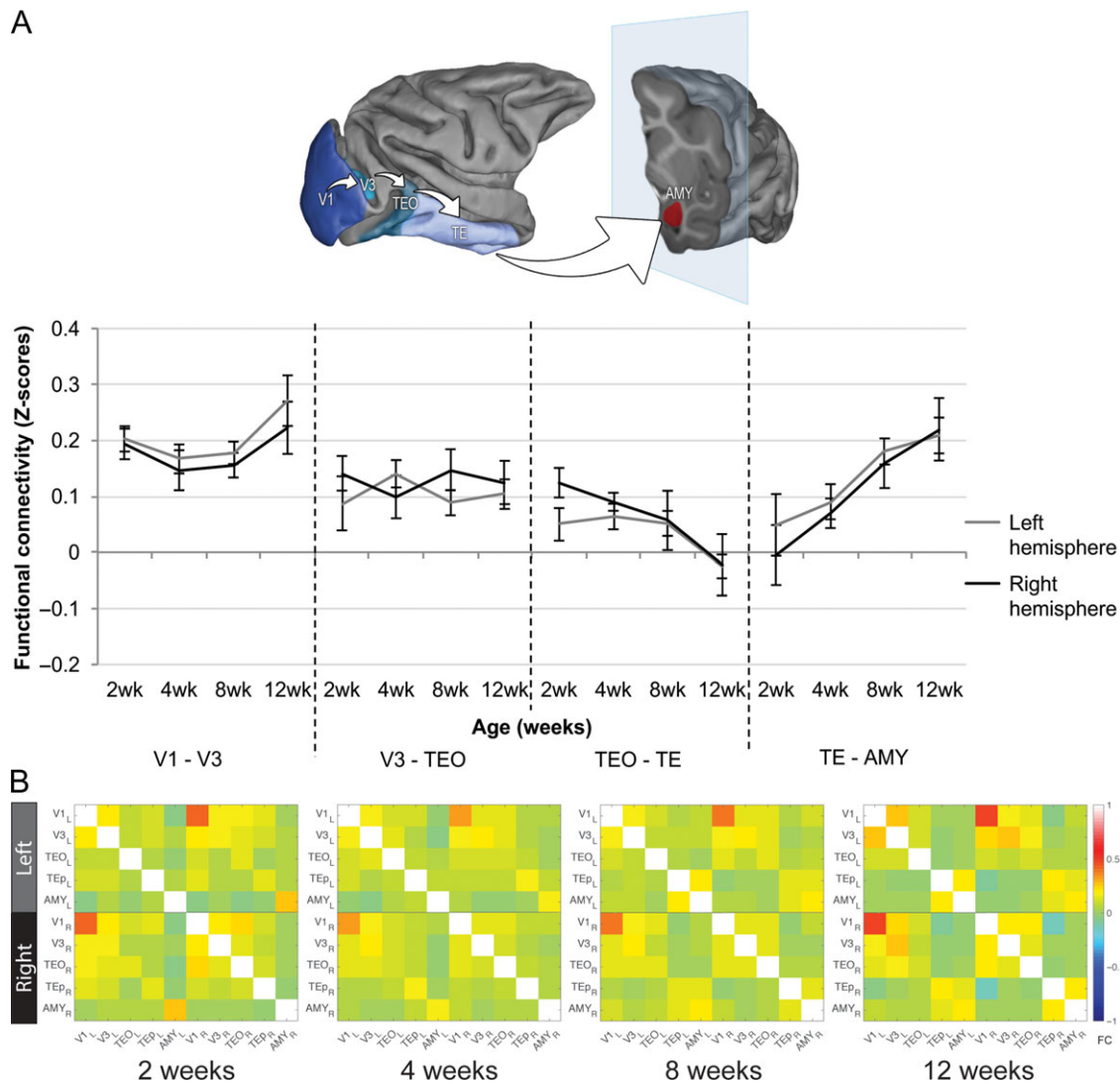
**Figure 1.** Functional connectivity (FC) within the ventral object pathway. (A) FC between the analyzed regions of interest (ROIs) in the two hemispheres separately. Blue shaded areas indicate ROIs analyzed along the ventral object pathway (V1–V3-TEO–TE–AMY), displayed on the Caret F99 macaque template (Van Essen 2002). TEO–TE: decreased FC from *week 2 to 12*, *week 4 to 12* and *week 8 to 12*; TE–AMY: increased FC from *week 2 to week 8 and 12*; and from *week 4 to week 12*. (B) FC matrices showing every possible ROI–ROI connectivity used for the network analysis within the ventral object pathway at each age point.

for detecting developmental changes and group differences in DTI fractional anisotropy using similar sample sizes as those used in this study was $d = 1.24$.

First, developmental changes in ROI–ROI FC (Fisher Z-transformed data) along each pathway were statistically analyzed using Repeated Measures Analysis of Variance (rmANOVA), in IBM SPSS Statistics (IBM Corporation, Armonk, NY, RRID: SCR_002 865) and R Studio (RStudio Inc, Boston, MA, RRID: SCR_000 432) with AGE [2, 4, 8, 12 weeks] and brain HEMISPHERE [left vs right] as repeated factors. Whenever a main or interaction effect was detected, post-hoc analyses were conducted using Tukey HSD tests to reveal group-wise differences.

Then, the network analysis was performed using an in-house built Matlab function to examine global developmental changes in FC separately for each pathway, using a Repeated Measures ANOVA model per functional system (ventral object pathway, ventral motion pathway, dorsal attention/spatio-visual pathways) with 5 ROIs per system and per hemisphere (left and right), and 4 longitudinal scans.

Significance level was set at $P < 0.05$ for both the ROI–ROI and network analyses. Data is reported as mean Fisher Z-transformed FC data ±SEM and effect sizes (effect sizes were available for the ROI–ROI, but not for the network analyses). Main effects of AGE (2, 4, 8 and 12 weeks) and LATERALITY (left, right; plus interhemispheric for the network analysis), and their interaction effects are reported below.

Although we standardized and kept the levels of isoflurane and telazol to the minimum necessary for sedation and below levels reported to affect FC in macaques (Vincent et al. 2007; Hutchison et al. 2013; Li et al. 2013; Tang and Ramani 2016), we also controlled for the potential confounding effect of anesthesia exposure on infant FC in a rmANCOVA model, adding anesthetic levels as time-variant covariates in the overall statistical model after checking whether they had a significant effect on our measures (effect sizes were not available for the rmANCOVA model).

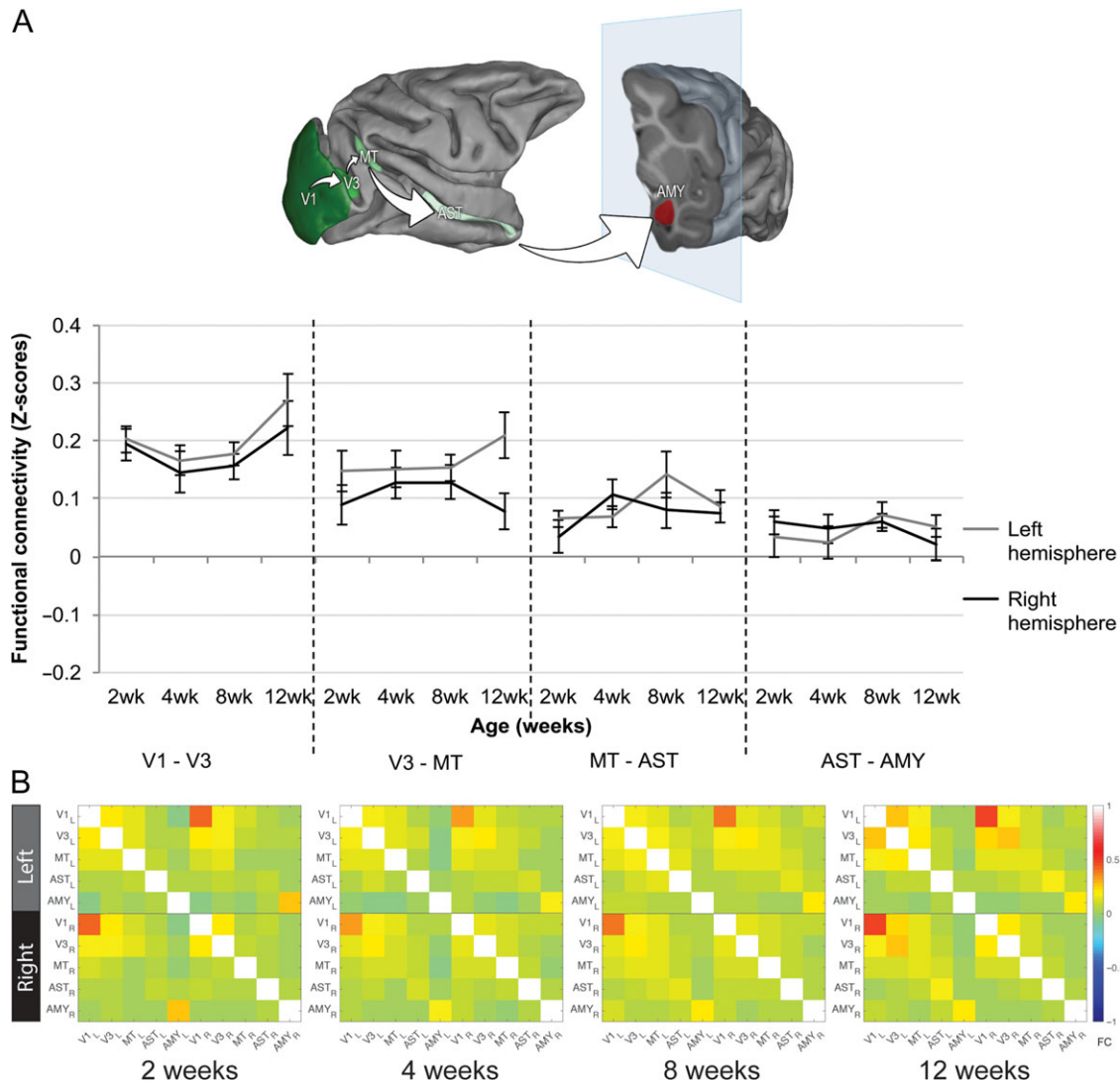The adolescent and adult awake-anesthesia comparison FC data were generated and presented in this paper only for

**Figure 2.** Functional connectivity (FC) within the ventral motion pathway. (A) FC between the analyzed regions of interest (ROIs) in the two hemispheres separately. Green shaded areas indicate ROIs analyzed along the ventral motion pathway, displayed on the Caret F99 macaque template (Van Essen 2002). From dark to light green: V1 – V3 – MT – AST – AMY. V3–MT: higher FC over the left hemisphere compared with the right; unchanged FC between MT–AST and AST–AMY during infancy. (B) FC matrices showing every possible ROI–ROI connectivity used for the network analysis within the ventral motion pathway at each age point.

qualitative comparisons with developmental FC data (i.e., they were not included in the rmANOVA statistical analysis, as the data were acquired in separate groups of animals). Both adolescent and adult data had considerable signal dropout in some ROIs (Adolescents: V1, TE; Adults: TE, TEO, FEF, BA46), which were excluded from the comparisons. Effects of anesthetics (isoflurane, telazol induction) on adolescent FC were also tested; no effects of isoflurane dose were found, although Pearson correlations detected dose effects of telazol on MT–AST ($r = 0.438$, $P = 0.020$), V3–LIP ($r = -0.433$, $P = 0.021$) and LIP–BA46 FC ($r = -0.571$, $P = 0.002$), which were excluded from the comparisons with infants. Note that telazol induction doses were higher in adolescents than in infants ($t(12) = 5.212$, $P < 0.001$).

## Results

### Ventral Object Pathway

As shown in Figure 1A, analysis of FC between ROIs along the ventral object pathway revealed strong FC between visual area V1 and visual area V3 already early after birth (at 2 weeks), with a slight increase after 8 weeks, in both hemispheres, although this age-related change did not reach statistical significance (AGE effect: $F(3,27) = 1.196$, $P = 0.33$, $\eta^2 = 0.12$). In both hemispheres, FC between V3 and TEO was weak, and remained stable as the infants became older (AGE effect: $F(3,27) = 0.013$, $P = 0.99$, $\eta^2 = 1.45 \times 10^{-3}$), showing similar levels than adolescent animals (average FC value: $0.15 \pm 0.03$). However, FC between inferior temporal areas TEO and TE showed a significant decrease with age, supported by a strong effect size (AGE effect: $F(3,27) = 6.046$, $P = 2.75 \times 10^{-3}$, $\eta^2 = 0.40$). Post-hoc Tukey HSD tests revealed significant decrease in FC at 12 weeks in comparison to all earlier ages (from 2 to 12 weeks: $P = 3.71 \times 10^{-3}$; 4 to 12 weeks: $P = 8.56 \times 10^{-3}$; 8 to 12 weeks: $P = 0.05$). In sharp contrast, analysis of the TE–AMY ROIs showed significant increases in FC with age, supported by a strong effect size (AGE effect: $F(3,27) = 7.909$, $P = 6.07 \times 10^{-4}$, $\eta^2 = 0.47$). Post hoc analyses showed that FC Z-values between these regions significantly increased from 2 to 8 and 12 weeks ($P < 0.01$), and from 4 to 12 weeks ($P < 0.05$).
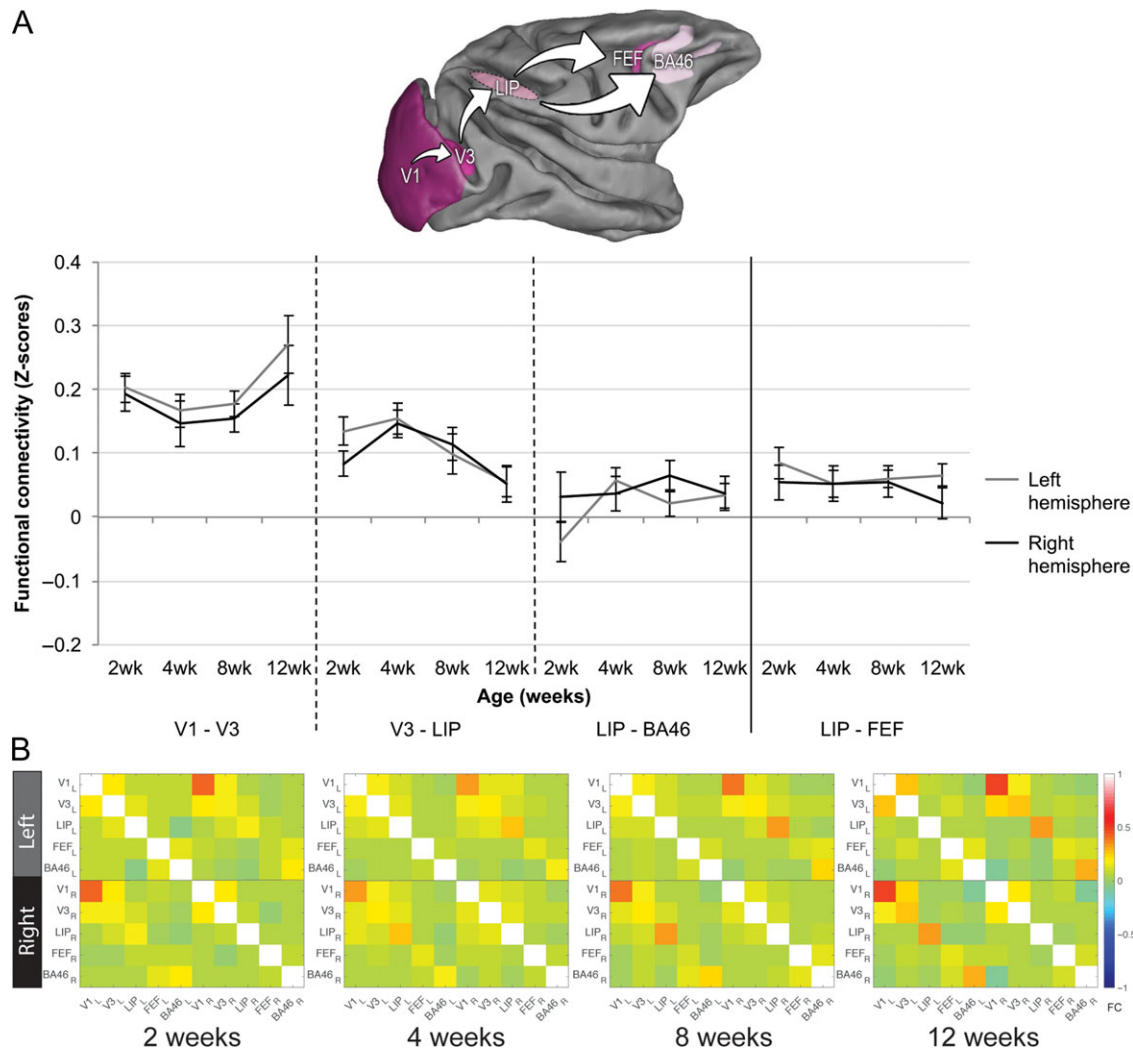
**Figure 3.** Functional connectivity (FC) within the dorsal attention/visuo-spatial pathways. (A) FC between the analyzed regions of interest (ROIs) in the two hemispheres separately. Pink shaded areas indicate ROIs analyzed along the dorsal visual-spatial pathway, displayed on the Caret F99 macaque template (Van Essen 2002). From dark to light pink: V1 – V3 – LIP – BA46 or FEF. V3–LIP: decreased FC from *week 4* to *week 12*; LIP–BA46: uncoupled ROIs during infancy. (B) FC matrices showing every possible ROI–ROI connectivity used for the network analysis within the dorsal attention/visuo-spatial pathways at each age point.

Although we kept isoflurane and telazol levels to the minimum possible, potential confounding effects of anesthetics on FC data were addressed by including them as covariates in the statistical models, when appropriate. Because a significant effect of telazol ($F(1,39) = 4.984$, $P = 0.03$) was detected on V1–V3 FC, telazol (measured as mg/kg BW) was included as a covariate in the statistical model. Controlling for telazol levels did not affect the findings, as the rmANCOVA analysis still did not reveal FC changes with age (AGE effect: $F(3,65) = 1.810$, $P = 0.15$). No other anesthetic effects were detected within the ventral object pathway.

Network analysis showed no significant global changes in FC with age within the ventral object pathway (AGE effect: $F(3,27) = 0.101$, $P = 0.96$; see Fig. 1B), suggesting that the developmental ROI–ROI FC changes reported above are ROI-specific. A significant HEMISPHERE effect ($F(2,18) = 181.01$, $P = 1.2 \times 10^{-12}$) followed by post hoc Tukey HSD showed stronger intra-hemispheric FC within the left hemisphere compared with the interhemispheric FC (difference: $-0.029 \pm 0.004$, $P = 9.71 \times 10^{-5}$), and within the right hemisphere compared with the interhemispheric FC (difference: $-0.025 \pm 0.008$, $P = 0.016$). However, FC

was similar within the left and the right hemispheres (difference: $-0.004 \pm 0.008$, $P = 0.889$) (Fig. 1B).

## Ventral Motion Pathway

Statistical results for FC in the caudal part of the ventral motion pathway (between V1 and V3) were presented in the previous section, although the graph is presented again in Figure 2A to include the entire pathway. As also shown in Figure 2A, there were no significant age-related changes in FC between V3 and MT or between MT and AST (AGE effect, V3–MT: $F(3,27) = 0.247$, $P = 0.86$, $\eta^2 = 0.03$; MT–AST: $F(3,27) = 2.398$, $P = 0.09$, $\eta^2 = 0.21$). However, FC was higher in the left hemisphere compared with the right across the first 3 months for V3–MT, with a strong effect size detected (HEMISPHERE effect: $F(1,9) = 9.107$, $P = 0.01$, $\eta^2 = 0.50$). When comparing infant data at the older age (12 weeks) with the adolescence reference values, we observed similar V3–MT FC in both age groups (Adolescent FC value: $0.17 \pm 0.02$). Finally, FC between AST and AMY was very weak in infants across the first 3 months of life (AGE effect: $F(3,27) = 0.087$, $P = 0.97$, $\eta^2 = 0.01$), but stronger in adolescents (average FC value:

0.15 ± 0.05) suggesting that FC between some regions along this pathway continues to increase after infancy.

Analyses were also performed to determine potential confounding effects of anesthetics on FC between ROIs within the ventral motion pathway. Although no isoflurane effects were found, a significant effect of telazol was detected on V3–MT FC ($F(1,42) = 6.93$, $P = 0.01$), which was included as a covariate in the statistical model, without affecting our main findings. Thus, even after controlling for this confounding effect of telazol, the rmANCOVA analysis did not reveal V3–MT FC changes with age (AGE effect: $F(3,66) = 0.579$, $P = 0.63$), but FC was stronger in left than right hemisphere (HEMISPHERE effect: $F(1,63) = 6.939$, $P = 0.01$). No other anesthetic effects were detected within the ventral motion pathway.

Network analysis showed no significant global changes in FC with age within the ventral motion pathway (AGE effect: $F(3,27) = 1.201$, $P = 0.33$; Fig. 2B). A significant HEMISPHERE effect ($F(2,18) = 334.86$, $P = 5.8 \times 10^{-15}$) followed by post hoc Tukey HSD showed FC differences between the left hemisphere and the interhemispheric FC (difference: $-0.021 \pm 0.004$, $P = 0.003$) as well as between the right hemisphere and the interhemispheric FC (difference: $-0.031 \pm 0.006$, $P = 0.002$) and between the left and right hemispheres (difference: $0.010 \pm 0.003$, $P = 0.05$). The analysis also revealed a trend towards unique hemispheric FC changes with age (AGE × HEMISPHERE interaction: $F(6,54) = 2.162$, $P = 0.06$), with FC decreasing in the left hemisphere from 4 to 8 weeks (difference: $-0.047 \pm 0.012$, $P = 0.02$), and different interhemispheric, left and right intrahemispheric FC values at 12 weeks of age (stronger left intrahemispheric FC compared with interhemispheric FC, difference: $-0.032 \pm 0.010$, $P = 0.02$; stronger right intrahemispheric FC compared with interhemispheric FC, difference: $-0.054 \pm 0.004$, $P = 8.8 \times 10-7$; and stronger right than left intrahemispheric FC, difference: $-0.022 \pm 0.008$, $P = 0.055$).

### Dorsal Attention/Visuo-spatial Pathways

As shown in Figure 3A, in the caudal part of the dorsal attention/visuo-spatial pathways, FC between V3–LIP weakened as the infants became older (AGE effect: $F(3,27) = 2.944$, $P = 0.05$, $\eta^2=0.25$). Post-hoc Tukey HSD test revealed a significant decrease in FC specifically from 4 to 12 weeks of age ($P = 0.03$). On the rostral part of this pathway, FC between LIP–BA46 remained weak at all infant ages tested (AGE effect: $F(3,27) = 1.138$, $P = 0.35$, $\eta^2=0.11$), and FC between LIP–FEF was also stable and weak during development (AGE effect: ($F(3,27) = 0.484$, $P = 0.70$, $\eta^2=0.05$). Unfortunately, no adolescent data was available for comparison with the infant FC in these pathways; however, the low adult V3–LIP FC reported below both under anesthesia and in the awake state indicates that FC between these two regions may remain low at later ages.

No confounding effects of anesthetics on FC were detected within the dorsal visual-spatial pathway.

Network analysis showed no significant global changes in FC with age within the dorsal attention/visuo-spatial pathways (AGE effect: $F(3,27) = 0.037$, $P = 0.99$; Fig. 3B). A significant HEMISPHERE effect ($F(2,18) = 304.52$, $P = 1.3 \times 10^{-14}$), followed by a post hoc Tukey HSD showed interhemispheric, left and right intrahemispheric FC differences for this pathway (stronger left intrahemispheric compared with interhemispheric FC, difference: $-0.021 \pm 0.002$, $P = 1.5 \times 10^{-5}$; stronger right intrahemispheric compared with interhemispheric FC, difference: $-0.034 \pm 0.003$, $P = 7.5 \times 10^{-7}$; and stronger right than left intrahemispheric FC, difference: $-0.013 \pm 0.004$, $P = 0.01$).

### Adult FC Comparison of Awake-anesthesia Condition Along the Studied Pathways

As expected based on reports in macaques (Vincent et al. 2007; Hutchison et al. 2013; Li et al. 2013; Tang and Ramani 2016), ROI–ROI FC values along the pathways studied were dampened compared with the awake condition [Awake condition: (V3–MT left: 0.29 ± 0.37, right: 0.30 ± 0.33; MT–AST left: 0.33 ± 0.19, right: 0.32 ± 0.36; AST–AMY left: 0.42 ± 0.32, right: 0.40 ± 0.25; V3–LIP left: 0.11 ± 0.20, right: −0.15 ± 0.12); Anesthesia condition: (V3–MT left: 0.11 ± 0.07, right: 0.10 ± 0.05; MT–AST left: 0.16 ± 0.06, right: 0.15 ± 0.03; AST–AMY left: 0.22 ± 0.11, right: 0.13 ± 0.06; V3–LIP left: 0.06 ± 0.04, right: 0.02 ± 0.02)]. The low FC values between some, but not all ROIs in infants were also low in adults even in the awake state (e.g., V3–LIP). But adult FC between other ROIs under anesthesia (e.g., AST–AMY), were much higher than in infants. Note that FC dampening effects of anesthesia in adults may be partially explained by the higher anesthetic levels used compared with infants. Altogether our data support that the low isoflurane levels (and induction anesthetics, such as telazol) used in our infant studies are below the threshold where FC seems affected in adults (Vincent et al. 2007; Hutchison et al. 2013; Li et al. 2013; Miranda-Dominguez 2014b; Tang and Ramani 2016).

## Discussion

Our findings showed region-specific maturational changes in FC between areas underlying social visual engagement in macaques (i.e., ventral object and motion pathways, dorsal attention/visuo-spatial pathways). Maturation along the visual pathways proceeds in a caudo-rostral progression with primary visual areas (V1–V3) developing earlier than higher-order visual and attentional areas (e.g., MT–AST, LIP–FEF).

The primary visual areas of the ventral object pathway support local feature detection, whereas the more rostral associative areas integrate these features to allow object and scene perception and recognition, with some cortical areas specialized in decoding social stimuli, such as faces (Desimone et al. 1984; Perrett et al. 1985; Tsao et al. 2003; Hadj-Bouziane et al. 2008; Pinsk et al. 2009; Ungerleider and Bell 2011). The strong V1–V3 FC found as early as 2 weeks of age suggests that local feature detection mediated by these areas develops very early, yet the slight FC increase between 8 and 12 weeks indicates progressive stronger coupling in activity patterns. In contrast, visual association cortices (TEO and TE) showed weaker FC, including moderate V3-TEO FC from 2 to 12 weeks. Thus, the weaker FC suggests that higher-order perceptual integration and object constancy mediated by these temporal regions mature later (Kovacs et al. 1999; Kovacs 2000). Finally, TE–AMY interactions are also critical for face identity and facial expressions (Gothard et al. 2007; Hoffman et al. 2007; Mosher et al. 2010; Schwiedrzik et al. 2015), which emerge in the first months in monkeys (Lutz et al. 1998; Kuwahata et al. 2004; Sugita 2008; Muschinski et al. 2016; Parr et al. 2016). Thus, the stronger TE–AMY coupling in the first 12 weeks of age may enable greater precision in the evaluation of social stimuli and faces in particular.

Cortical areas along the motion pathway detect body motion as well as facial and eye motion from expressions. FC between V3–MT and MT–AST was moderate but stable during the first 3 months. By 12 weeks, V3–MT FC was similar to that observed in the adolescent brain. By contrast, MT–AST FC slightly increased (trend) between 2 and 12 weeks suggesting further maturation

of FC after 3 months. This developmental pattern is in line with the emergence of detection of motion direction around 2 weeks (Kiorpes and Movshon 2004; Kiorpes et al. 2012), which continues to improve during the first 3 months to reach adult-like levels by 3 years (Mikami and Fujita 1992). Further, the ability to rapidly evaluate direct-gaze faces emerges by 3 months (Mendelson et al. 1982; Muschinski et al. 2016).

Areas within the dorsal visual pathway are intimately involved in the control of oculomotor and spatially-directed attention (Milner and Goodale 1995). V3–LIP FC progressively decreased between 4 and 12 weeks of age to reach levels observed in adults by 3 months; however, the weak V3–LIP FC suggests slow maturation of visuo-spatial abilities in monkeys as it does in human infants until 10–12 months of age (Braddick and Atkinson 2011). It is not surprising to have found weak FC between the parietal and prefrontal areas (LIP–BA46, LIP–FEF) during the first 3 months of age, as stronger coupling of these areas may emerge only in late adolescence (Conde et al. 1996). Unfortunately, we don't have data in adolescents or adults to support this prediction.

## Mechanisms Underlying FC Changes

The specific mechanisms that underlie FC changes in visual cortical areas in early infancy are still poorly understood and remain speculative. Nevertheless, the progressive coupling in activity patterns between the most caudal cortical areas V1–V3 between 8 and 12 weeks is consistent with the synaptic proliferation and rapid dendritic spine increase observed in many cortical areas during the first 3 months of life (Rakic et al. 1986). It also parallels the sharp increase in metabolic activity reported in the most caudal visual areas from 2 to 4 months of age (Bachevalier et al. 1991; Distler et al. 1996), as well as the presence of adult-like selective responsivity of neurons within V1 and MT in awake infant monkeys only a few weeks old (Rodman et al. 1993). By contrast, FC between higher order association areas of all visual pathways (TEO–TE, MT–AST, LIP–BA46/FEF) were weaker even at 3 months of age. Again, these findings are in line with those of previous histological studies showing that these cortical areas are metabolically immature at birth, reaching adult-like metabolic levels around 3 months of age (Distler et al. 1996). Furthermore, as compared with adults, single unit studies of young infant monkeys indicated lower magnitudes of visual responses in TE (Rodman et al. 1993) and slower pattern-motion responses in MT neurons (Movshon et al. 2004; Kiorpes et al. 2007). Together, the available data is consistent with the recent demonstration of the presence of a retinotopic proto-organization of the infero-temporal visual cortex at birth, which serves as scaffolding for subsequent category-selective organization (Arcaro and Livingstone 2017). Indeed, studies involving face-deprived monkeys indicate that face experience is necessary for the formation of face domains (Arcaro et al. 2017) and that early visual experience is crucial for normal visual cortical development during infancy.

Lastly, the increase in TE–AMY FC between 2 and 12 weeks in monkeys may relate to observations of progressive retraction of exuberant projections from TE to AMY (Webster et al., 1991; Webster, Bachevalier and Ungerleider, personal communication). This anatomical refinement of connections, presumably due to experience, could increase the functional strength of remaining TE inputs to AMY neurons. Together with significant volumetric increase and morphological changes – including myelination – within the AMY during the first 3 months postpartum in monkeys (Payne et al. 2010; Chareyron et al. 2012),

the fine-tuning of TE–AMY connections may enable greater precision in the evaluation of social stimuli and faces in particular.

## Study Limitations

First, although scans were acquired under low levels of anesthesia to minimize isoflurane effects on BOLD signal, potential FC differences could still exist with awake states. Some brain networks FC (default mode -DMN-, sensorimotor, visual, etc.) seem modulated by levels of consciousness clinically described by arousal and awareness (Boly et al. 2008; Guldenmund et al. 2012; Heine et al. 2012). Thus, little or no changes in DMN adult connectivity was found during awareness (awake state) or moderate sedation, but reduced connectivity occurred during anesthesia (altered state of awareness with low wakefulness), and no differences existed during light sleep (decreased awareness) or sedation. In the present study, the isoflurane levels used were below those employed in previous macaque publications reporting patterns of coherent BOLD fluctuations under anesthesia similar to the awake state, including in sensory and visual systems (Vincent et al. 2007; Hutchison et al. 2013; Li et al. 2013; Tang and Ramani 2016). Furthermore, controlling for anesthetic levels as covariates in the statistical models did not change FC results in any pathways, supporting the reliability of the findings. Yet, the effects of anesthesia on FC cannot be entirely ignored, especially on immature brains. Indeed, when compared with our findings, Arcaro and Livingstone (2017) showed strong FC between V2/V3 and more rostral visual areas when infant monkeys were asleep and not anesthetized. Also, single unit recordings in TE and STS result in only a paucity of visually responsive neurons in young anesthetized (nitrous oxide) infant monkeys, whereas the number of visually responsive neurons is similar to that of adult monkeys when recordings are done on awake infant monkeys (Rodman et al. 1993).

Second, only male subjects were used in this study to avoid potential sex differences in brain development and increase our sample size, but also to assess neurodevelopmental changes of social visual networks important for ASD-related social deficits where the prevalence rate is much greater in males than females (Christensen et al. 2016).

Third, the focus on infants from middle-ranking families may mask potential individual variability in brain maturation across the social hierarchy. Therefore, future studies are needed to establish the developmental trajectories at later ages (>3 months), across the whole social hierarchy and in females, and to identify physiological/cellular/molecular mechanisms responsible for FC changes during development.

## Relevance to Human Visual System Development

Abundant knowledge has been gathered on the development of human visual function (e.g., Braddick and Atkinson 2011; Klaver et al. 2011), yet little is known on the brain changes that underlie such maturational processes especially in the first months of life. Neuroimaging studies in human infants so far suggest parallel development of visual cortical areas supporting early social skills in both humans and monkeys. For example, both PET and fMRI studies showed (1) maturation of primary visual areas (V1/V2/V3) early in life (Chugani and Phelps 1986; Chugani et al. 1987; Gao et al. 2015), (2) presence of unique resting state networks, including primary visual cortex, sensorimotor areas, and lateral parietal cortex in infant brain (Fransson et al. 2007) and (3) emergence of FC between primary visual cortex and higher-order visual areas during infancy – neonates to

2 years (Deen et al. 2016; Lin et al. 2008). These human findings suggest that visual neural networks are just beginning to develop during infancy as they do in monkeys. Given the difficulty in scanning typically developing human infants, our findings are highly valuable to better understand the normative development of social visual networks in humans.

## Funding

## Notes

## References

Andersson JL, Skare S, Ashburner J. 2003. How to correct susceptibility distortions in spin-echo echo-planar images: application to diffusion tensor imaging. Neuroimage. 20: 870–888.

Arcaro MJ, Livingstone MS. 2017. A hierarchical, retinotopic proto-organization of the primate visual system at birth. Elife. 6:e26196.

Arcaro MJ, Schade PF, Vincent JL, Ponce CR, Livingstone MS. 2017. Seeing faces is necessary for face-domain formation. Nat Neurosci. 20:1404–1412.

Bachevalier J, Hagger C, Mishkin M. 1991. Functional maturation of the occipitotemporal pathway in infant rhesus monkeys. In: Alfred Benzon Symposium No. 31: Brain Work and Brain Function, Munksgaard, Copenhagen, p. 231–240.

Baylis GC, Rolls ET, Leonard CM. 1987. Functional subdivisions of the temporal lobe neocortex. J Neurosci. 7:330–342.

Boly M, Phillips C, Tshibanda L, Vanhaudenhuyse A, Schabus M, Dang-Vu TT, Moonen G, Hustinx R, Maquet P, Laureys S. 2008. Intrinsic brain activity in altered states of consciousness: how conscious is the default mode of brain function? Ann N Y Acad Sci. 1129:119–129.

Boussaoud D, Ungerleider LG, Desimone R. 1990. Pathways for motion analysis: cortical connections of the medial superior temporal and fundus of the superior temporal visual areas in the macaque. J Comp Neurol. 296:462–495.

Braddick O, Atkinson J. 2011. Development of human visual function. Vision Res. 51:1588–1609.

Burgess GC, Kandala S, Nolan D, Laumann TO, Power JD, Adeyemo B, Harms MP, Petersen SE, Barch DM. 2016. Evaluation of denoising strategies to address motion-correlated artifacts in resting-state functional magnetic resonance imaging data from the Human Connectome Project. Brain Connect. 6:669–680.

Casey BJ, Giedd JN, Thomas KM. 2000. Structural and functional brain development and its relation to cognitive development. Biol Psychol. 54:241–257.

Chareyron LJ, Lavenex PB, Amaral DG, Lavenex P. 2012. Postnatal development of the amygdala: a stereological study in macaque monkeys. J Comp Neurol. 520:1965–1984.

Christensen DL, Baio J, Braun KV, Bilder D, Charles J, Constantino MD, Daniels J, Durkin MS, Fitzgerald RT, Kurzius-Spencer M, et al. 2016. Prevalence and characteristics of autism spectrum disorder among children aged 8 years—autism and developmental disabilities monitoring network, 11 Sites, United States, 2012. Surveillance Summaries. 65:1–23.

Chugani HT, Phelps ME. 1986. Maturational changes in cerebral function in infants determined by 18FDG positron emission tomography. Science. 231:840–843.

Chugani HT, Phelps ME, Mazziotta JC. 1987. Positron emission tomography study of human brain functional development. Ann Neurol. 22:487–497.

Ciric R, Wolf DH, Power JD, Roalf DR, Baum GL, Ruparel K, Shinohara RT, Elliott MA, Eickhoff SB, Davatzikos C, et al. 2017. Benchmarking of participant-level confound regression strategies for the control of motion artifact in studies of functional connectivity. Neuroimage. 154:174–187.

Conde F, Lund JS, Lewis DA. 1996. The hierarchical development of monkey visual cortical regions as revealed by the maturation of parvalbumin-immunoreactive neurons. Brain Res Dev Brain Res. 96:261–276.

Damon F, Meary D, Quinn PC, Lee K, Simpson EA, Paukner A, Suomi SJ, Pascalis O. 2017. Preference for facial averageness: evidence for a common mechanism in human and macaque infants. Sci Rep. 7:46303.

Dean DC 3rd, O'Muircheartaigh J, Dirks H, Waskiewicz N, Lehman K, Walker L, Han M, Deoni SC. 2014. Modeling healthy male white matter and myelin development: 3 through 60months of age. Neuroimage. 84:742–752.

Deen B, Richardson H, Dilks DD, Takahashi A, Keil B, Wald LL, Kanwisher N, Saxe R. 2016. Organization of high-level visual cortex in human infants. Nature Comm. doi:10.1038/ncomms13995.

Deoni SC, Mercure E, Blasi A, Gasston D, Thomson A, Johnson M, Williams SC, Murphy DG. 2011. Mapping infant brain myelination with magnetic resonance imaging. J Neurosci. 31:784–791.

Deoni SC, O'Muircheartaigh J, Elison JT, Walker L, Doernberg E, Waskiewicz N, Dirks H, Piryatinsky I, Dean DC 3rd, Jumbe NL. 2016. White matter maturation profiles through early childhood predict general cognitive ability. Brain Struct Funct. 221:1189–1203.

Desimone R, Albright TD, Gross CG, Bruce C. 1984. Stimulus-selective properties of inferior temporal neurons in the macaque. J Neurosci. 4:2051–2062.

Diagnostic and Statistical Manual of Mental Disorders (DSM-5). Fifth Edition. 2013. American Psychiatric Association.

Dickinson AR, Calton JL, Snyder LH. 2003. Nonspatial saccade-specific activation in area LIP of monkey parietal cortex. J Neurophysiol. 90:2460–2464.

Distler C, Bachevalier J, Kennedy C, Mishkin M, Ungerleider LG. 1996. Functional development of the corticocortical pathway

for motion analysis in the macaque monkey: a 14C-2-deoxyglucose study. Cereb Cortex. 6:184–195.

Fair DA, Cohen AL, Power JD, Dosenbach NU, Church JA, Miezin FM, Schlaggar BL, Petersen SE. 2009. Functional brain networks develop from a "local to distributed" organization. PLoS Comput Biol. 5:e1000381.

Fair DA, Dosenbach NUF, Church JA, Cohen AL, Brahmbhatt S, Miezin FM, Barch DM, Raichle ME, Petersen SE, Schlaggar BL. 2007. Development of distinct control networks through segregation and integration. Proc Natl Acad Sci U S A. 104:13507–13512.

Fair DA, Nigg JT, Iyer S, Bathula D, Mills KL, Dosenbach NU, Schlaggar BL, Mennes M, Gutman D, Bangaru S, et al. 2012. Distinct neural signatures detected for ADHD subtypes after controlling for micro-movements in resting state functional connectivity MRI data. Front Syst Neurosci. 6:80.

Fransson P, Skiold B, Horsch S, Nordell A, Blennow M, Lagercrantz H, Aden U. 2007. Resting-state networks in the infant brain. Proc Natl Acad Sci U S A. 104:15531–15536.

Furl N, Hadj-Bouziane F, Liu N, Averbeck BB, Ungerleider LG. 2012. Dynamic and static facial expressions decoded from motion-sensitive areas in the macaque monkey. J Neurosci. 32:15952–15962.

Gao W, Alcauter S, Elton A, Hernandez-Castillo CR, Smith JK, Ramirez J, Lin W. 2015. Functional network development during the first year: relative sequence and socioeconomic correlations. Cereb Cortex. 25:2919–2928.

Gao W, Zhu H, Giovanello KS, Smith JK, Shen D, Gilmore JH, Lin W. 2009. Evidence on the emergence of the brain's default network from 2-week-old to 2-year-old healthy pediatric subjects. Proc Natl Acad Sci U S A. 106:6790–6795.

Geng X, Gouttard S, Sharma A, Gu H, Styner M, Lin W, Gerig G, Gilmore JH. 2012. Quantitative tract-based white matter development from birth to age 2 years. Neuroimage. 61:542–557.

Godfrey JR, Diaz MP, Pincus M, Kovacs-Balint Z, Feczko E, Earl E, Miranda-Dominguez O, Fair D, Sanchez MM, Wilson ME, et al. 2018. Diet matters: glucocorticoid-related neuroadaptations associated with calorie intake in female rhesus monkeys. Psychoneuroendocrinology. 91:169–178.

Gorgolewski K, Burns CD, Madison C, Clark D, Halchenko YO, Waskom ML, Ghosh SS. 2011. Nipype: a flexible, lightweight and extensible neuroimaging data processing framework in python. Front Neuroinform. 5:13.

Gothard KM, Battaglia FP, Erickson CA, Spitler KM, Amaral DG. 2007. Neural responses to facial expression and face identity in the monkey amygdala. J Neurophysiol. 97:1671–1683.

Grayson DS, Bliss-Moreau E, Machado CJ, Bennett J, Shen K, Grant KA, Fair DA, Amaral DG. 2016. The rhesus monkey connectome predicts disrupted functional networks resulting from pharmacogenetic inactivation of the amygdala. Neuron. 91:453–466.

Guldenmund P, Vanhaudenhuyse A, Boly M, Laureys S, Soddu A. 2012. A default mode of brain function in altered states of consciousness. Arch Ital Biol. 150:107–121.

Hadj-Bouziane F, Bell AH, Knusten TA, Ungerleider LG, Tootell RB. 2008. Perception of emotional expressions is independent of face selectivity in monkey inferior temporal cortex. Proc Natl Acad Sci U S A. 105:5591–5596.

Heine L, Soddu A, Gomez F, Vanhaudenhuyse A, Tshibanda L, Thonnard M, Charland-Verville V, Kirsch M, Laureys S, Demertzi A. 2012. Resting state networks and consciousness: alterations of multiple resting state network connectivity in physiological, pharmacological, and pathological consciousness States. Front Psychol. 3:295.

Hoffman KL, Gothard KM, Schmid MC, Logothetis NK. 2007. Facial-expression and gaze-selective responses in the monkey amygdala. Curr Biol. 17:766–772.

Howell BR, McCormack KM, Grand AP, Sawyer NT, Zhang X, Maestripieri D, Hu X, Sanchez MM. 2013. Brain white matter microstructure alterations in adolescent rhesus monkeys exposed to early life stress: associations with high cortisol during infancy. Biol Mood Anxiety Disord. 3:21.

Hutchison RM, Womelsdorf T, Gati JS, Everling S, Menon RS. 2013. Resting-state networks show dynamic functional connectivity in awake humans and anesthetized macaques. Hum Brain Mapp. 34:2154–2177.

Iyer SP, Shafran I, Grayson D, Gates K, Nigg JT, Fair DA. 2013. Inferring functional connectivity in MRI using Bayesian network structure learning with a modified PC algorithm. Neuroimage. 75:165–175.

Kiorpes L, Hawken MJ, Movshon JA, Kohn A, Rust NC. 2007. What does MT contribute to the development of sensitivity to visual motion. Perception. 36:10–11. (ECVP Abstract Supplement).

Kiorpes L, Movshon JA. 2004. Development of sensitivity to visual motion in macaque monkeys. Vis Neurosci. 21:851–859.

Kiorpes L, Price T, Hall-Haro C, Movshon JA. 2012. Development of sensitivity to global form and motion in macaque monkeys (Macaca nemestrina). Vision Res. 63:34–42.

Klaver P, Marcar V, Martin E. 2011. Neurodevelopment of the visual system in typically developing children. Prog Brain Res. 189:113–136.

Klin A, Jones W, Schultz R, Volkmar F, Cohen D. 2002. Visual fixation patterns during viewing of naturalistic social situations as predictors of social competence in individuals with autism. Arch Gen Psychiatry. 59:809–816.

Klin A, Lin DJ, Gorrindo P, Ramsay G, Jones W. 2009. Two-year-olds with autism orient to non-social contingencies rather than biological motion. Nature. 459:257–261.

Klin A, Shultz S, Jones W. 2015. Social visual engagement in infants and toddlers with autism: early developmental transitions and a model of pathogenesis. Neurosci Biobehav Rev. 50:189–203.

Knickmeyer RC, Gouttard S, Kang C, Evans D, Wilber K, Smith JK, Hamer RM, Lin W, Gerig G, Gilmore JH. 2008. A structural MRI study of human brain development from birth to 2 years. J Neurosci. 28:12176–12182.

Kovacs I. 2000. Human development of perceptual organization. Vision Res. 40:1301–1310.

Kovacs I, Kozma P, Feher A, Benedek G. 1999. Late maturation of visual spatial integration in humans. Proc Natl Acad Sci USA. 96:12204–12209.

Kuwahata H, Adachi I, Fujita K, Tomonaga M, Matsuzawa T. 2004. Development of schematic face preference in macaque monkeys. Behav Processes. 66:17–21.

Lewis JW, Van Essen DC. 2000. Corticocortical connections of visual, sensorimotor, and multimodal processing areas in the parietal lobe of the macaque monkey. J Comp Neurol. 428:112–137.

Li CX, Patel S, Auerbach EJ, Zhang X. 2013. Dose-dependent effect of isoflurane on regional cerebral blood flow in anesthetized macaque monkeys. Neurosci Lett. 541:58–62.

Lin W, Zhu Q, Gao W, Chen Y, Toh CH, Styner M, Gerig G, Smith JK, Biswal B, Gilmore JH. 2008. Functional connectivity MR

imaging reveals cortical functional connectivity in the developing brain. AJNR Am J Neuroradiol. 29:1883–1889.

Liu Y, Yttri EA, Snyder LH. 2010. Intention and attention: different functional roles for LIPd and LIPv. Nat Neurosci. 13: 495–500.

Lutz CK, Lockard JS, Gunderson VM, Grant KS. 1998. Infant monkeys' visual responses to drawings of normal and distorted faces. Am J Primatol. 44:169–174.

Machado CJ, Bachevalier J. 2003. Non-human primate models of childhood psychopathology: the promise and the limitations. J Child Psychol Psychiatry. 44:64–87.

Maltbie EA, Kaundinya GS, Howell LL. 2017. Ketamine and pharmacological imaging: use of functional magnetic resonance imaging to evaluate mechanisms of action. Behav Pharmacol. 28:610–622.

Markov NT, Ercsey-Ravasz MM, Ribeiro Gomes AR, Lamy C, Magrou L, Vezoli J, Misery P, Falchier A, Quilodran R, Gariel MA, et al. 2014. A weighted and directed interareal connectivity matrix for macaque cerebral cortex. Cereb Cortex. 24:17–36.

McLaren DG, Kosmatka KJ, Kastman EK, Bendlin BB, Johnson SC. 2010. Rhesus macaque brain morphometry: a methodological comparison of voxel-wise approaches. Methods. 50: 157–165.

McLaren DG, Kosmatka KJ, Oakes TR, Kroenke CD, Kohama SG, Matochik JA, Ingram DK, Johnson SC. 2009. A population-average MRI-based atlas collection of the rhesus macaque. Neuroimage. 45:52–59.

Mendelson MJ, Haith MM, Goldmanrakic PS. 1982. Face scanning and responsiveness to social cues in infant rhesus-monkeys. Dev Psychol. 18:222–228.

Mikami A, Fujita K. 1992. Development of the ability to detect visual motion in infant macaque monkeys. Dev Psychobiol. 25:345–354.

Milner AD, Goodale MA 1995. The visual brain in action. Oxford: Oxford University Press.

Miranda-Dominguez O, Mills BD, Carpenter SD, Grant KA, Kroenke CD, Nigg JT, Fair DA. 2014a. Connectotyping: model based fingerprinting of the functional connectome. PLoS One. 9:e111048.

Miranda-Dominguez O, Mills BD, Grayson D, Woodall A, Grant KA, Kroenke CD, Fair DA. 2014b. Bridging the gap between the human and macaque connectome: a quantitative comparison of global interspecies structure-function relationships and network topology. J Neurosci. 34:5552–5563.

Mosher CP, Zimmerman PE, Gothard KM. 2010. Response characteristics of basolateral and centromedial neurons in the primate amygdala. J Neurosci. 30:16197–16207.

Movshon JA, Rust NC, Kohn A, Kiorpes L, Hawken MJ. 2004. Receptive field properties of MT neurons in infant macaques. Perception. 33:27. (ECVP Abstract Supplement).

Murphy K, Fox MD. 2017. Towards a consensus regarding global signal regression for resting state functional connectivity MRI. Neuroimage. 154:169–173.

Muschinski J, Feczko E, Brooks JM, Collantes M, Heitz TR, Parr LA. 2016. The development of visual preferences for direct versus averted gaze faces in infant macaques (*Macaca mulatta*). Dev Psychobiol. 58:926–936.

Nalci A, Rao BD, Liu TT. 2017. Global signal regression acts as a temporal downweighting process in resting-state fMRI. Neuroimage. 152:602–618.

O'Muircheartaigh J, Dean DC 3rd, Ginestet CE, Walker L, Waskiewicz N, Lehman K, Dirks H, Piryatinsky I, Deoni SC. 2014. White matter development and early cognition in babies and toddlers. Hum Brain Mapp. 35:4475–4487.

Parr LA. 2011. The evolution of face processing in primates. Philos Trans R Soc Lond B Biol Sci. 366:1764–1777.

Parr LA, Murphy L, Feczko E, Brooks J, Collantes M, Heitz TR. 2016. Experience-dependent changes in the development of face preferences in infant rhesus monkeys. Dev Psychobiol. 58:1002–1018.

Passingham R. 2009. How good is the macaque monkey model of the human brain? Curr Opin Neurobiol. 19:6–11.

Paxinos G, Huang X, Toga AW 1999. The Rhesus Monkey Brain in Stereotaxic Coordinates. London, UK: Academic Press.

Payne C, Machado CJ, Bliwise NG, Bachevalier J. 2010. Maturation of the hippocampal formation and amygdala in *Macaca mulatta*: a volumetric magnetic resonance imaging study. Hippocampus. 20:922–935.

Perrett DI, Smith PA, Potter DD, Mistlin AJ, Head AS, Milner AD, Jeeves MA. 1985. Visual cells in the temporal cortex sensitive to face view and gaze direction. Proc R Soc Lond B Biol Sci. 223:293–317.

Pinsk MA, Arcaro M, Weiner KS, Kalkus JF, Inati SJ, Gross CG, Kastner S. 2009. Neural representations of faces and body parts in macaque and human cortex: a comparative FMRI study. J Neurophysiol. 101:2581–2600.

Power JD, Barnes KA, Snyder AZ, Schlaggar BL, Petersen SE. 2012. Spurious but systematic correlations in functional connectivity MRI networks arise from subject motion. Neuroimage. 59:2142–2154.

Power JD, Laumann TO, Plitt M, Martin A, Petersen SE. 2017. On global fMRI signals and simulations. Trends Cogn Sci. 21: 911–913.

Power JD, Mitra A, Laumann TO, Snyder AZ, Schlaggar BL, Petersen SE. 2014. Methods to detect, characterize, and remove motion artifact in resting state fMRI. Neuroimage. 84:320–341.

Preuss TM. 2000. Taking the measure of diversity: comparative alternatives to the model-animal paradigm in cortical neuroscience. Brain Behav Evol. 55:287–299.

Rakic P, Bourgeois JP, Eckenhoff MF, Zecevic N, Goldman-Rakic PS. 1986. Concurrent overproduction of synapses in diverse regions of the primate cerebral cortex. Science. 232: 232–235.

Rodman HR, Scalaidhe SP, Gross CG. 1993. Response properties of neurons in temporal cortical visual areas of infant monkeys. J Neurophysiol. 70:1115–1136.

Rodman HR, Skelly JP, Gross CG. 1991. Stimulus selectivity and state dependence of activity in inferior temporal cortex of infant monkeys. Proc Natl Acad Sci U S A. 88:7572–7575.

Saleem KS, Logothetis NK 2012. A Combined MRI and Histology Atlas of the Rhesus Monkey Brain in Stereotaxic Coordinates. London, UK: Academic Press.

Schwiedrzik CM, Zarco W, Everling S, Freiwald WA. 2015. Face patch resting state networks link face processing to social cognition. PLoS Biol. 13:e1002245.

Scott JA, Grayson D, Fletcher E, Lee A, Bauman MD, Schumann CM, Buonocore MH, Amaral DG. 2016. Longitudinal analysis of the developing rhesus monkey brain using magnetic resonance imaging: birth to adulthood. Brain Struct Funct. 221: 2847–2871.

Scott LS, Pascalis O, Nelson CA. 2007. A domain-general theory of the development of perceptual discrimination. Curr Dir Psychol Sci. 16:197–201.

Seltzer MM, Krauss MW, Shattuck PT, Orsmond G, Swe A, Lord C. 2003. The symptoms of autism spectrum disorders in adolescence and adulthood. J Autism Dev Disord. 33: 565–581.

Shi Y, Budin F, Yapuncich E, Rumple A, Young J, Payne C, Zhang X, Hu X, Godfrey J, Howell B, et al. 2017. UNC-Emory Infant atlases for macaque brain image analysis: postnatal brain development through 12 months. Front Neurosci. 10: 617.

Smith SM, Jenkinson M, Woolrich MW, Beckmann CF, Behrens TE, Johansen-Berg H, Bannister PR, De Luca M, Drobnjak I, Flitney DE, et al. 2004. Advances in functional and structural MR image analysis and implementation as FSL. Neuroimage. 23(Suppl 1):S208–S219.

Styner M, Knickmeyer R, Joshi S, Coe C, Short SJ, Gilmore J. 2007. Automatic brain segmentation in rhesus monkeys. Med Imaging 2007: Image Process, Pts 1–3. 6512:L5122.

Sugita Y. 2008. Face perception in monkeys reared with no exposure to faces. Proc Natl Acad Sci U S A. 105:394–398.

Suomi SJ. 2005. Mother-infant attachment, peer relationships, and the development of social networks in rhesus monkeys. Hum Dev. 48:67–79.

Suomi SJ. 2006. Risk, resilience, and gene x environment interactions in rhesus monkeys. Ann N Y Acad Sci. 1094:52–62.

Tang CY, Ramani R. 2016. fMRI and anesthesia. Int Anesthesiol Clin. 54:129–142.

Tsao DY, Freiwald WA, Knutsen TA, Mandeville JB, Tootell RB. 2003. Faces and objects in macaque cerebral cortex. Nat Neurosci. 6:989–995.

Ungerleider LG, Bell AH. 2011. Uncovering the visual "alphabet": advances in our understanding of object perception. Vision Res. 51:782–799.

Ungerleider LG, Mishkin M. 1982. Two cortical visual systems. In: Ingle DG, editor. Analysis of visual behavior. Cambridge, MA: MIT Press. p. 549–586.

Van Essen DC. 2002. Windows on the brain: the emerging role of atlases and databases in neuroscience. Curr Opinion Neurobiol. 12:574–579.

Vincent JL, Patel GH, Fox MD, Snyder AZ, Baker JT, Van Essen DC, Zempel JM, Snyder LH, Corbetta M, Raichle ME. 2007. Intrinsic functional architecture in the anaesthetized monkey brain. Nature. 447:83–86.

Wang A, Payne C, Moss S, Jonesteller T, Wesson J, Jones W, Parr LA, Bachevalier J 2017. Development of social-visual engagement in Rhesus Macaques (*Macaca mulatta*). 47th Annual Meeting of the Society for Neuroscience (SFN). Washington, DC. Nov. 11–15. Program No. 588.26.

Webster MJ, Ungerleider LG, Bachevalier J. 1991. Connections of inferior temporal areas TE and TEO with medial temporal-lobe structures in infant and adult monkeys. J Neurosci. 11: 1095–1116.

Woolrich MW, Jbabdi S, Patenaude B, Chappell M, Makni S, Behrens T, Beckmann C, Jenkinson M, Smith SM. 2009. Bayesian analysis of neuroimaging data in FSL. Neuroimage. 45:S173–S186.

Yan CG, Cheung B, Kelly C, Colcombe S, Craddock RC, Di Martino A, Li Q, Zuo XN, Castellanos FX, Milham MP. 2013. A comprehensive assessment of regional variation in the impact of head micromovements on functional connectomics. Neuroimage. 76:183–201.